32×32 OPTICAL PHASED ARRAY WITH ULTRA-LIGHTWEIGHT HIGH-CONTRAST-GRATING MIRRORS

B. W. Yoo[1], M. Megens[1,2], T. K. Chan[2], T. Sun[1], W. Yang[1], D. A. Horsley[2], C. J. Chang-Hasnain[1], and M. C. Wu[1]*
[1]University of California, Berkeley, CA, USA
[2]University of California, Davis, CA, USA

ABSTRACT

Optical phased arrays (OPA) with fast response time are of great interest for various applications such as displays, free space optical communications, and laser radar. In this paper, we report on a novel 32×32 OPA with fast response time (<4 microseconds), large field of view (±2°), and narrow beam divergence (0.1°). This is made possible by integrating ultra-lightweight high-contrast-grating (HCG) mirrors with high-speed electrostatic actuators in a dense two-dimensional array with high fill-factor. Consisting of a thin layer (400nm) of sub-wavelength polysilicon gratings, the HCG mirror has a high reflectivity (99.9%), a broad reflection bandwidth, and weighs only 140pg.

KEYWORDS

Optical phased array (OPA), beamsteering, micro-electro-mechanical systems (MEMS), lightweight, high contrast grating (HCG)

INTRODUCTION

Optical phased arrays (OPA) [1,2] are versatile beamforming devices for many applications such as laser radar (ladar), free-space laser communications, 3D holographic displays, and high-resolution 3D imaging [3,4]. The OPA imposes a phase profile on the incoming beam through a two-dimensional (2D) array of phase shifters. It can be programmed to generate multiple simultaneous beams, allowing precise pointing, tracking, and stabilization of multiple targets. It also offers random-access pointing and dynamic focusing/defocusing capabilities. The OPA is usually much faster than a single steering mirror as individual phase shifters are much smaller and more nimble than the large scanning mirror.

Liquid crystal OPAs have been extensively reported since the initial demonstration using liquid crystal television panels [5,6]. However, their operation speed is slow because it takes tens of milliseconds for an electric field to reorient the molecules of the liquid crystal. Because the liquid crystal basis in OPAs is a continuous medium, it does not display the required phase pattern in the flyback region, where phase changes from 2π to 0. In addition, liquid crystal materials tend to be highly temperature sensitive, restricting their application area.

An alternative technology for OPAs is MEMS [7,8]. Phase shifters can be realized by "piston" mirrors. Typical MEMS mirrors are made of metal-coated single- or polycrystalline silicon, or multi-layer distributed Bragg reflectors. Though faster than bulk mirrors, the mass of the mirrors still limits the operational speed of MEMS-based OPAs. Moreover, the thermally induced bi-layer stress often causes mirrors to warp, affecting optical performance. The residual absorption in the metal also limits the maximum optical power before catastrophic damage occurs.

In this paper, we demonstrate an ultrafast MEMS OPA with ultra-lightweight high-contrast-grating (HCG) mirrors. The HCG mirror consists of a thin layer (400nm) of sub-wavelength gratings. It has high reflectivity (~99.9%) and broad bandwidth [9,10]. The mass of a 20×20 μm^4 HCG mirror is 140g, about ~100× lighter than a semiconductor distributed Bragg reflector (DBR) of comparable reflectivity. Thanks to its lightweight, the resonant frequency can be increased up to ~MHz. Since gratings are made of a single material, the HCG-OPAs have potential to operate at high optical power without damage or warping due to thermal expansion mismatch.

MODELING

The layout of our MEMS OPA with HCG mirrors is shown in Figure 1. The array size of the OPA is 32×32. Anchors of adjacent HCGs in the same column are shared. The spacing between springs and HCG elements is defined to be close to our DUV stepper lithography limit (250 nm), resulting in a fill-factor of 85%. Electrical fan-out is connected to 32 bonding pads allowing for one-dimensional beamsteering.

Figure 2 shows the SEM image of the low-stress polysilicon HCG mirror suspended by four mechanical springs made in the same polysilicon layer (300 nm wide and 18 μm long). The area of the HCG mirror is 20×20 μm^2 and pixel-to-pixel spacing (Λ) is 22 μm, resulting in a maximum scan angle of $\theta=\pm sin^{-1}(\lambda_0/2\Lambda)=\pm 2°$ for λ_0 = 1550 nm wavelength.

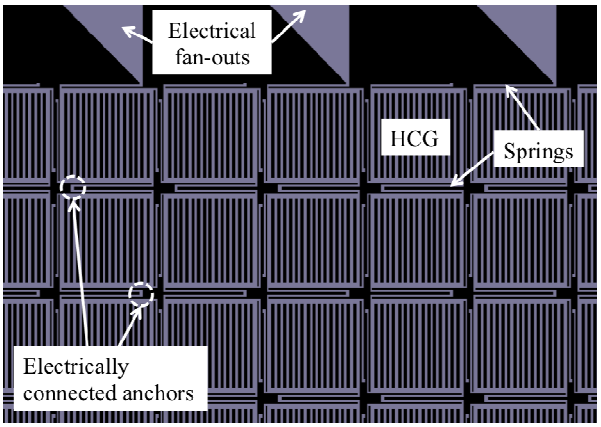

Figure 1: Layout of the MEMS optical phased array. Anchors of HCG mirrors electrically connect adjacent mirrors in the same row, increasing fill-factor.

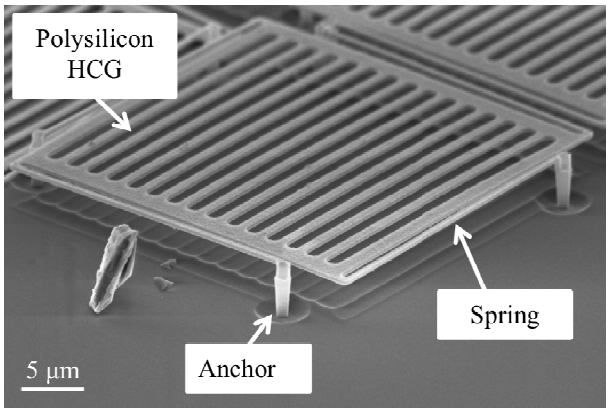

Figure 2: Scanning electron microscope (SEM) image of a polysilicon high contrast sub-wavelength grating (HCG). The pixel surface is extremely flat due to the low stress 400 nm polysilicon structural layer, suitable for beamsteering applications using 1550 nm wavelength.

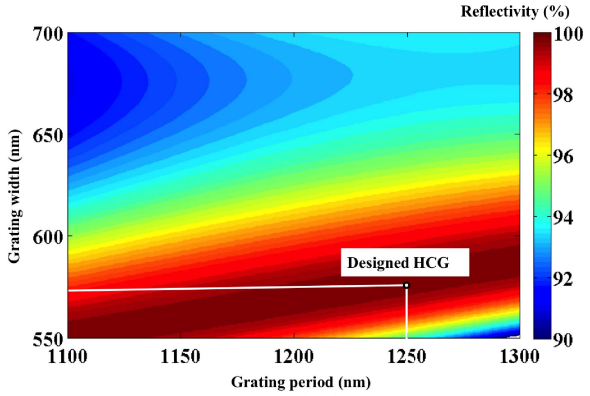

Figure 3: FDTD simulation result of HCG reflectivity versus period and bar width showing a reflectivity of 99.93%.

Figure 3 illustrates the HCG reflectivity contours in transverse electric (TE) mode with respect to the period and width of the grating bars in the HCG. In the near-wavelength regime, where the grating period is between λ/n_r and λ/n_a (n_r is refractive index of grating bars and n_a is refractive index of air), extraordinary features of HCGs such as high reflectivity (~99.9%) and high quality-factor resonance ($Q>10^7$) have been recently explored [11]. In addition to the periodic design of gratings in the near-wavelength regime as above, highly reflective HCG can be realized, provided that a selected high index medium for gratings is designed to be surrounded by low index materials. Figure 3 shows that the reflectivity of HCGs can feature higher than 99.9% based on Finite-difference time-domain (FDTD) method. The designed HCG has a period of 1250nm and a bar width of 570nm, producing very high reflectivity. The fabrication tolerance of the bar width is designed to be more than ±10nm which is achievable by DUV lithography.

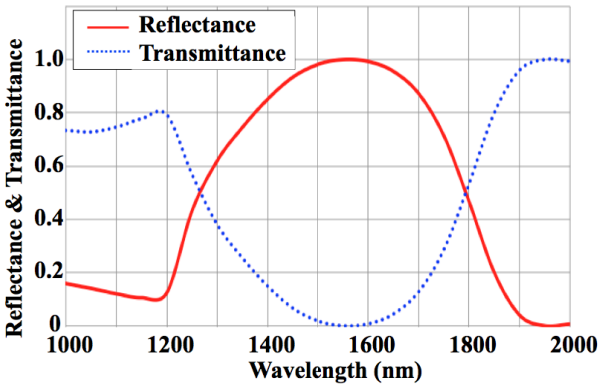

Figure 4: Theoretical Reflectance and transmittance spectra of the HCG mirror.

The broad reflection bandwidth of the HCG is a result of the high index contrast between the grating bars and the surrounding medium. The reflectivity is higher than 99% in the range from 1517nm to 1605nm as shown in Figure 4. Reflectivity over 99.9% can be achieved from 1548nm to 1575nm.

FABRICATION

We fabricate a HCG OPA on a silicon substrate. The fabrication process is illustrated in Figure 5(a) Low temperature oxide (LTO) is deposited and annealed in a furnace. (b) Anchoring holes of 0.5 μm diameter are formed using a DUV stepper and a dry etcher. (c) Stoichiometric silicon nitride is thinly deposited in the furnace. Silicon nitride is used as anchor material not only to electrically isolate substrate and device layer, but also to survive in the release process using hydrofluoric (HF) acid. (d) Removal of backside dielectric follows to reveal the contact for grounding. The top silicon nitride is removed using chemical-mechanical–polishing (CMP), allowing for low temperature oxide to be sacrificial layer as well as actuation gap. Then, polysilicon is deposited and CMPed to smoothen the surface of the HCG reflectors, resulting in high reflectivity. (e) DUV stepper and dry etching are used to define HCGs, springs, and anchors. (f) Diluted HF remove the sacrificial LTO and release phased arrays.

The SEM image of a fabricated 32×32 OPA is shown in Figure 6. Here, the pixels in the same column are electrically linked via their anchors for one-dimensional beam scanning. The CMPed polysilicon is only 400 nm thick, resulting in an ultra-lightweight (140 pg) mirror with a high resonant frequency of 0.46 MHz. Buffered HF is used for stable etch rate, but attacks phosphorous doped polysilicon and results in lower resonant frequency. Diluted HF works better for release and leads to 0.46 MHz, in good agreement with theory.

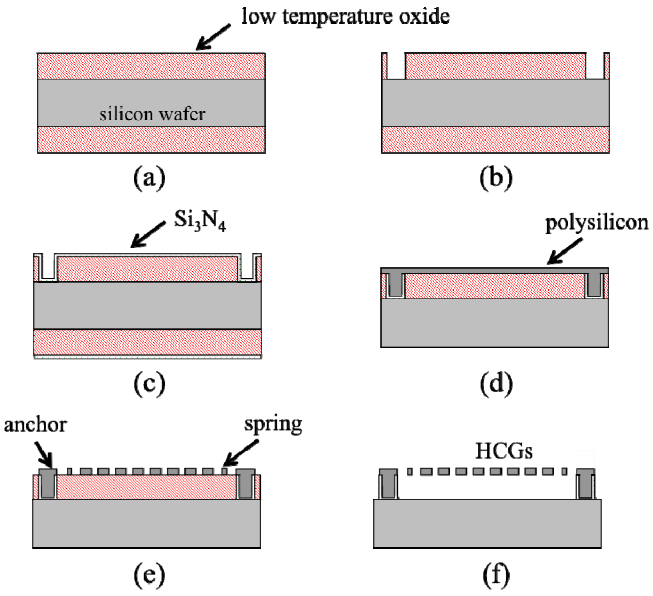

Figure 5: Fabrication process.

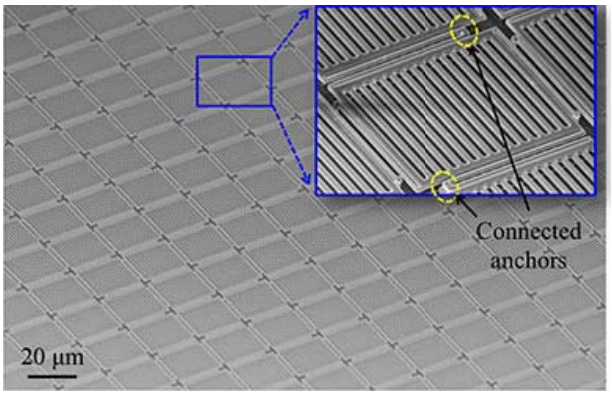

Figure 6: SEM image of the fabricated HCG phase shifter array. Inset shows that anchors in the same column are linked to adjacent HCGs via mechanical springs for one-dimensional beamsteering. This can be extended to two-dimension beamforming by adding multi-layer interconnects underneath the HCG mirrors.

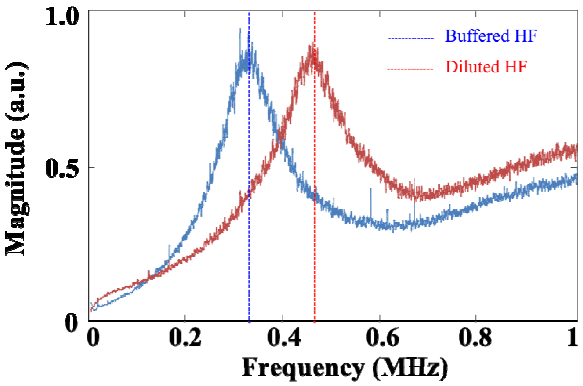

Figure 7: Experimental resonant frequencies of an HCG using a laser Doppler vibrometer (LDV) system. A HCG released in diluted HF depicts the measured resonant frequency is 0.46 MHz, which agrees well with the theory.

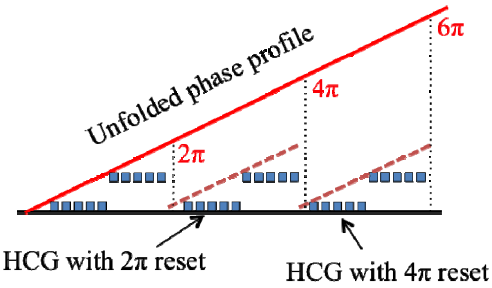

Figure 8: Modulo 2π phase shifting using HCGs to create beamsteering at maximum angle. Light is in the form of a sine wave. Thus, 2nπ (n=0,1,2…), from a phase point of view, are all the same so that a stair-step ramp approach can be used to steer light.

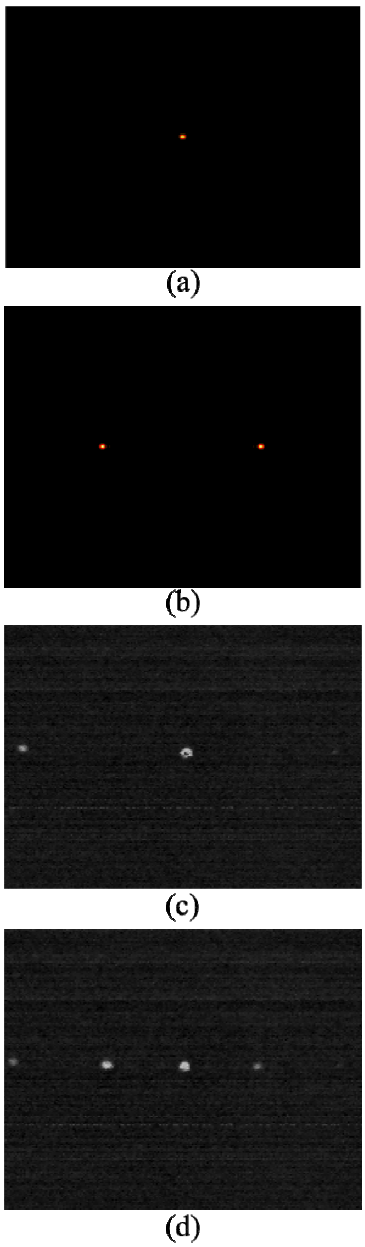

Figure 9: Beamsteering simulation results (a, b) and measurement results (c, d) in the far field. (a) without bias and (b) beamsteering in simulation. (c) without bias and (d) beamsteering in the far-field. Maximum steered angle is ± 2°.

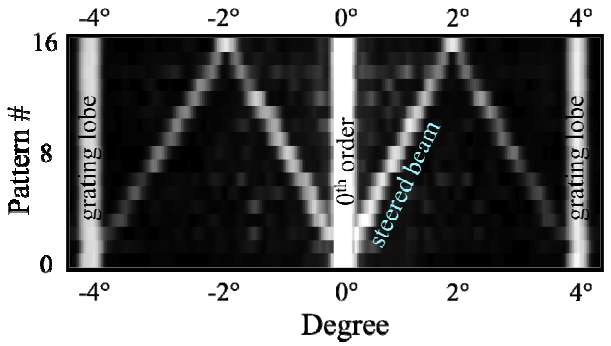

Figure 10: Measured intensity of steered beams. 17 patterns are shown from beams at rest to steered beams at maximum angle (maximum phase shift of ~0.4π).

BEAMSTEERING DEMONSTRATION

Light could be steered by using a prism. But monochromatic light is a sine wave so that a modulo 2π phase profile can be employed for beamsteering using OPAs to efficiently approximate the optical path difference (OPD) of a prism [2]. A stair-step ramp approach allows for a modulo 2π phase profile and is shown in Figure 8. The maximum angle is achieved when HCGs alternates between 0π and 1π phase shift. Figures 9(a) and (b) illustrate the simulated far-field patterns at rest and at the maximum beamsteering angle, respectively. Figures 9(c) and (d) show the corresponding experimental measurements. In Figure 9(c), as no voltage is applied, the 0-th order beam is very strong; grating lobes are also observable at the end of the field of view. In Figure 9(d), we see the steered beams appear. The measured deflection angle is ±2°, matching well with the simulation result. The intensity of the measured 0-th order beam is stronger than the simulation, because the phase shift is less than π radians. Figure 10 depicts the measured intensity of steered beams, aiming on steering the 0-th order beam (pattern #0) to 16 different angles until reaching the maximum angle. The beam intensity for maximum steerable angle (pattern #16) corresponds to Figure 9(d). Since phase shift in the beamsteering demonstration is kept below 0.4π for stable actuation, the intensity of the measured beam at maximum angle is only 1/3 of the potential maximum beam intensity. The rest of this power appears in the 0-th order beam and the grating lobes. This is expected to improve when applying full π phase shift.

CONCLUSIONS

In conclusions, a 32×32 optical phased array with ultra-lightweight (140 pg) high-contrast-grating (HCG) mirrors and high fill-factor (85%) has been demonstrated to perform ±2° beamsteering with fast response time (<4 microseconds) and narrow beam divergence (0.1°).

The high reflectivity, nearly zero absorption, and single-material construction of the HCG mirrors make this phased array an attractive candidate for high-energy laser applications.

ACKNOWLEDGEMENTS

This project is supported by DARPA SWEEPER program (No. HR0011–10–2–0002).

REFERENCES

[1] J. Sun, E. Timurdogan, A. Yaacobi, E.S. Hosseini, and M.R. Watts, "Large-scale nanophotonic phased array," *Nature*, vol. 493, pp. 195-199, 2013.

[2] P.F. McManamon, P.J. Bos, M.J. Escuti, J. Heikenfeld, S. Serati, H. Xie, and E.A. Watson, "A review of phased array steering for narrow-band electrooptical systems," *Proc. IEEE.*, vol. 97, pp. 1078-1096, 2009.

[3 J.K. Doylend, M.J.R. Heck, J.T. Bovington, J.D. Peters, L.A. Coldren, and J.E. Bowers, "Two-dimensional free-space beam steering with an optical phased array on silicon-on-insulator," *Opt. Express,* vol. 19, pp. 21595-21604, 2011.

[4] P.F. McManamon, "Optical phased array technology, " *Proc. IEEE*, vol. 84, 268-298, 1996.

[5] D. Engström, M.J. O'Callaghan, C. Walker, and M.A. Handschy, "Fast beam steering with a ferroelectric-liquid-crystal optical phased array," *Appl. Opt.*, vol. 48, pp. 1721-1726, 2009.

[6] H.C. Jau, T.H. Lin, R.X. Fung, S.Y. Huang, J.H. Liu, and A.Y. Fuh, "Optically-tunable beam steering grating based on azobenzene doped cholesteric liquid crystal," *Opt. Express,* vol. 18, pp.17498-17503, 2010.

[7] T.G. Bifano, J. Perreault, R.K. Mail, and M.N. Horenstein, "Microelectromechanical deformable mirrors," *IEEE J. Sel. Top. Quant. Electron.*, vol. 5, pp. 83-89, 1999.

[8] U. Krishnamoorth, K. Li, K. Yu, D. Lee, J.P. Heritage, and O. Solgaard, "Dual-mode micromirrors for optical phased array applications," *Sens. Actuators A Phys*., vol. 97-98, pp. 21-26, 2002.

[9] M.C.Y. Huang, Y. Zhou, and C.J. Chang-Hasnain, "A surface-emitting laser incorporating a high-index-contrast sub-wavelength grating," *Nature Photon.*, vol. 1, pp. 119-122, 2007.

[10] B.W. Yoo, M. Megens, T.K. Chan, T. Sun, W. Yang, C.J. Chang-Hasnain, D.A. Horsley, and M.C. Wu, "Optical phased array using high contrast gratings for 2D beamforming and beamsteering," *Opt. Express*, in press.

[11] V. Karagodsky, and C. J. Chang-Hasnain, "Physics of near-wavelength high contrast grating", *Opt. Express*, vol. 20, pp. 10888-10895, 2012.